Journal of Organometallic Chemistry, 479 (1994) 237–245

An unprecedented tridentate mode of co-ordination of a BINAP ligand: synthesis and crystal structures of $[Ru(\eta^5\text{-}C_5H_5)\{(R)\text{-}(BINAP)\}]^+CF_3SO_3^-$ and $Ru(\eta^5\text{-}C_5H_5)\{(R)\text{-}(BINAP)\}I$

Devendra D. Pathak, Harry Adams, Neil A. Bailey, Philip J. King and Colin White

Department of Chemistry, The University, Sheffield S3 7HF (UK)

(Received December 13, 1993)

Abstract

The syntheses and crystal structures of the title compounds are reported. The complex $[Ru(\eta^5\text{-}C_5H_5)\{(R)\text{-}(BINAP)\}]^+CF_3SO_3^-$ is of particular interest in that it contains a tridentate BINAP ligand co-ordinated to the ruthenium through η^2-bonding to one of the naphthyl rings as well as through both phosphorus atoms. The possible implications of this type of bonding are discussed.

Key words: Ruthenium; Crystal structure; Polydentate; Triflate; Cyclopentadienyl; BINAP

1. Introduction

The ligand 2,2′-bis(diphenylphosphino)-1,1′-binaphthyl (BINAP) has proved to be one of the most effective chiral bis(phosphine) ligands for use in enantioselective synthesis [1]. In particular, ruthenium BINAP complexes have been shown to hydrogenate prochiral unsaturated carboxylic acids [2], oximes [3], allylic alcohols [4] and functionalised ketones [5], including β-keto esters [6], giving up to 100% ee. Prompted by a recent report on the synthesis and chemistry of $Ru(C_5H_5)\{(S)\text{-}(-)\text{-BINAP}\}Cl$ [7] we describe herein our studies of the chemistry of the related $Ru(C_5H_5)\{R\text{-}(+)\text{-BINAP}\}I$ including the true nature of the cationic species $[Ru(C_5H_5)(BINAP)]^+$.

2. Results and discussion

2.1. Synthetic studies

$Ru(C_5H_5)\{(R)\text{-BINAP}\}I$ (**1**) was readily prepared in 63% overall yield from $Ru_3(CO)_{12}$ *via* $Ru(C_5H_5)(CO)_2H$ by the *one-pot* procedure we have previously described for compounds of this type [8]. The crystal structure of **1** is shown in Fig. 1. Whilst investigating the chemistry of this compound we attempted to prepare the solvent complex $[Ru(\eta^5\text{-}C_5H_5)\{(R)\text{-BINAP}\}(ClCD_2Cl)]CF_3SO_3$ by the standard procedure of treating **1** with $Ag[CF_3SO_3]$ in CD_2Cl_2 and we were surprised by the spectroscopic properties of the product **2** we obtained. For example, in the ^1H NMR spectrum the pattern in the aromatic region was very different from that of **1**, with signals at much higher field, *e.g.* 6.20–5.90 (m, 4 H, Ar *H*). More striking was the difference in the ^{31}P spectra between **1** and the product. Thus, **1** showed two signals at δ 42.8 and 52.3 with $J_{PAPB} = 51.7$ Hz, which is not too dissimilar to the spectrum reported for $Ru(C_5H_5)\{(S)\text{-BINAP}\}Cl$ [7]. In contrast, the spectrum of **2** showed two signals with a large chemical shift difference between them, *i.e.* δ 14.1 and 74.0 with $J_{PAPB} = 43.7$ Hz. Intrigued by this, we repeated the halide abstraction reaction on a preparative scale and determined the crystal structure of the product **2**.

2.2. Description of structures

The bond lengths and angles with estimated standard deviations for the structure of $Ru(C_5H_5)\{(R)\text{-BINAP}\}I$ (**1**) are given in Table 2. A disordering of a toluene solvent molecule within a pocket in the lattice restricts the accuracy of the structure; attempts to

Correspondence to: Dr. C. White.

0022-328X/94/$7.00
SSDI 0022-328X(94)24433-J

© 1994 – Elsevier Science S.A. All rights reserved

model the apparent disorder gave no significant improvement over a single ordered solvent site, although the absence of a clear image in the electron density map does not support such an ordered model.

The cyclopentadienyl ligand is asymmetrically bonded (deviation of ruthenium atom 1.862 Å) and the Ru–I bond length of 2.745(2) Å is within the normal range of 2.72–2.78 Å found in other ruthenium(II) complexes [9]. Similarly, the Ru–P bond lengths lie between those found in $Ru(C_5H_4CH_3)\{(S)$-BINAP$\}Cl$ [7] and $[Ru(C_6H_6)\{(S)$-BINAP$\}Cl$ [10]. However, whereas the latter two complexes have a *skew* angle (the dihedral angle between the two naphthyl planes) of 78.0° and 75.7(2)°, the corresponding angle in (**1**) is significantly smaller at 66°. This is close to the extreme lower limit previously observed for BINAP complexes [11]. With the reduction in the *skew* angle there is a concomitant reduction in the bite angle of the BINAP ligand, *i.e.* $P_1–Ru–P_2 = 87.6°$; this compares with 91.6(1)° and 91.4(1)° observed in $Ru(C_5H_4CH_3)\{(S)$-BINAP$\}Cl$ [7] and $[Ru(C_6H_6)\{(S)$-BINAP$\}Cl$ [10] respectively. Presumably, this reflects the increased steric crowding in the iodo complex compared to the corresponding chloro complexes. The two pairs of terminal phenyl rings are inclined at 82 and 79°. Also the two six-membered rings of each naphthyl unit are planar and hinged at only 2.2 and 4.1°. The most striking aspect of the structure is that each naphthyl fragment lies approximately parallel to a terminal phenyl on the other phosphorus (13 and 19°), with mean interplanar separations for both pairs of 3.31 Å: the planar fragments are approximately eclipsed, with the phenyl positioned above the junction bond of the naphthyl. Thus, it appears that the molecular conformation is stabilised by intramolecular π-stacking.

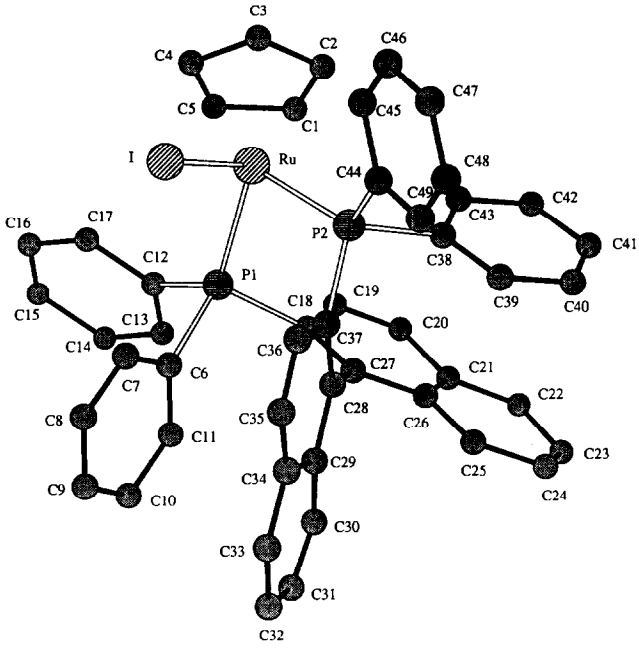

Fig. 1. Molecular structure of $Ru(C_5H_5)\{(R)$-BINAP$\}I$ (**1**).

There are no significant intermolecular contacts involving either the ruthenium complex or the solvent toluene.

The structure of the molecular cation is illustrated in Fig. 2; bond lengths and angles with estimated standard deviations are given in Table 4.

The cation comprises of a BINAP ligand bonded to a cyclopentadienyl-ruthenium fragment (r.m.s. deviation of the cyclopentadienyl ring 0.009 Å, deviation of ruthenium atom 1.899 Å). The apparent co-ordinative unsaturation of the ruthenium has been compensated by bonding to two adjacent carbon atom [C(25) and C(30)] of one of the naphthalene residues of the BINAP ligand (at 2.26 and 2.28 Å respectively). The corresponding distances in the second residue are 3.35 Å to C(36) and 3.21 Å to C(35); in the related neutral iodo complex **1**, the contacts to carbons adjacent to phosphorus lie at 3.32 and 3.53 Å. Contacts to carbons in the bond linking the naphthalene residues are in excess of 4 Å in both **1** and **2**. As expected the η^2-bonding to one of the six-membered rings of a naphthyl residue in **2** not only increases the bond distance between the two bound carbon fragments [*i.e.* C(25)–C(30) = 1.464(14) Å] but also disrupts the aromaticity of the co-ordinated ring. Thus, the bond length of C(26)–C(27) at 1.334(16) Å is in keeping with an isolated alkene bond, whereas the adjacent C(25)–C(26) and C(27)–C(28) bond lengths of 1.468(15) Å and 1.467(16) Å more closely resemble single bonds. The *skew* angle of the BINAP ligand has increased to 80° from the 66° observed for the corresponding iodo complex **1**. This presumably facilitates the η^2-bonding to the naphthyl residue but it is still comparable to the *skew* angle observed for other BINAP complexes [7,10,11]. In fact it is striking how little the BINAP ligand has to distort in order to bond *via* the naphthyl backbone as well as through the two phosphorus atoms.

The four terminal phenyl rings of the cation are each planar (r.m.s. deviations 0.004, 0.013, and 0.018, 0.011 Å) and the pairs are both inclined at 93°. Similarly, the two six-membered rings of each naphthalene unit are approximately coplanar and hinged at 4.2 and 2.5°.

The anion is triflate, in which each of S(1) and C(50) has a staggered, tetrahedral geometry, with enlarged O–S–O angles (mean 115.0°) and reduced F–C–F angles (mean 106.1°). There are no significant intermolecular contacts.

To our knowledge, the mode of bonding of the

TABLE 1. Atom coordinates ($\times 10^4$) and temperature factors ($Å^2 \times 10^3$) for Ru(C_5H_5){(*R*)-(+)-BINAP}I (1)

Atom	*x*	*y*	*z*	U_{eq} [a]
Ru(1)	0	−2627(1)	3952(1)	54(1)
I(1)	560(1)	−1696(1)	5434(1)	78(1)
P(1)	1190(3)	−3617(3)	3758(3)	47(1)
P(2)	763(3)	−1634(3)	3029(3)	51(1)
C(1)	−1072(8)	−3331(9)	3209(9)	101(11)
C(2)	−982	−3717	4079	84(9)
C(3)	−1201	−3047	4721	80(8)
C(4)	−1427	−2247	4249	90(10)
C(5)	−1347	−2422	3314	84(9)
C(6)	2317(6)	−3602(7)	4243(7)	55(6)
C(7)	2524	−3108	5009	63(6)
C(8)	3372	−3186	5397	77(8)
C(9)	4014	−3758	5020	97(10)
C(10)	3808	−4252	4253	81(8)
C(11)	2959	−4174	3865	56(6)
C(12)	964(8)	−4798(6)	4082(8)	56(6)
C(13)	1264	−5531	3581	80(8)
C(14)	1197	−6398	3935	103(10)
C(15)	829	−6532	4789	125(13)
C(16)	529	−5798	5289	78(8)
C(17)	597	−4931	4936	77(8)
C(18)	1409(10)	−3670(10)	2532(11)	52(5)
C(19)	848(12)	−4206(12)	1999(14)	74(7)
C(20)	898(10)	−4283(10)	1101(11)	52(5)
C(21)	1534(11)	−3722(11)	650(11)	62(6)
C(22)	1626(17)	−3749(16)	−300(14)	90(9)
C(23)	2269(19)	−3192(15)	−689(11)	89(9)
C(24)	2715(14)	−2579(13)	−259(13)	74(7)
C(25)	2653(13)	−2577(11)	695(12)	66(7)
C(26)	2046(10)	−3100(9)	1160(11)	48(5)
C(27)	1979(10)	−3087(9)	2123(10)	43(5)
C(28)	2456(10)	−2413(10)	2641(10)	49(5)
C(29)	3435(11)	−2457(10)	2712(11)	54(6)
C(30)	3936(10)	−3127(11)	2334(12)	55(6)
C(31)	4773(13)	−3212(13)	2473(14)	76(7)
C(32)	5301(13)	−2579(13)	2991(16)	82(8)
C(33)	4844(13)	−1891(15)	3400(14)	84(8)
C(34)	3860(11)	−1848(10)	3303(11)	55(6)
C(35)	3396(11)	−1191(10)	3749(11)	55(6)
C(36)	2475(11)	−1142(10)	3689(10)	46(5)
C(37)	1993(11)	−1725(9)	3105(10)	51(5)
C(38)	573(6)	−1660(7)	1820(5)	45(5)
C(39)	1087	−1116	1252	66(7)
C(40)	919	−1103	331	64(7)
C(41)	237	−1633	−23	92(9)
C(42)	−277	−2176	544	77(8)
C(43)	−109	−2190	1465	57(6)
C(44)	565(7)	−409(5)	3244(8)	62(6)
C(45)	−240	−187	3675	54(6)
C(46)	−477	713	3794	67(7)
C(47)	91	1390	3482	66(7)
C(48)	896	1168	3051	85(9)
C(49)	1132	269	2932	92(9)
C(50)	5487	−2855	−443	262(11)
C(51)	5917	−2459	283	262(11)
C(52)	6778	−2106	178	262(11)
C(53)	7209	−2150	−655	262(11)
C(54)	6778	−2546	−1383	262(11)
C(55)	5917	−2899	−1277	262(11)
C(56)	5442	−3336	−2081	262(11)

[a] Equivalent isotropic *U* defined as one third of the trace of the orthogonalised U_{ij} tensor.

BINAP ligand in **2** in which the BINAP ligand acts as tridentate ligand, co-ordinating through both phosphorus atoms and a η^2-naphthalene ring, is unprecedented. It also explains the upfield shift of some of the aromatic protons observed in the ^{1}H NMR spectrum of **2** since this is a characteristic feature of co-ordinated aromatic moieties [12]. We note that the previously reported $[RuH(BINAP)_2]PF_6$ is formally co-ordinatively unsaturated [13]. From the reported spectroscopic data it is not possible to reach any definite conclusion but we speculate that this molecule is a prime candidate to also contain a tridentate BINAP ligand.

The intriguing question is whether the tridentate co-ordination mode of BINAP observed in **2** plays any part in the catalytic chemistry of BINAP. For example, it has been suggested that agostic hydrogen interactions play a crucial role in $[Co(C_5Me_5)\{P(OMe)_3\}Et]^+$-catalysed oligomerisation reactions. They form in the "resting state" of the catalyst when there is no substrate in the immediate vicinity of the co-ordination site and open up when a substrate molecule is available; in this way they maintain the necessary vacant co-ordination site for the catalysis to proceed [14]. Given the ease of formation of **2** one could imagine that η^2-co-ordination to the binaphthalene backbone of BINAP also stabilises the "resting state" of the catalyst. If this is true, then as well as being formed readily, these additional η^2-co-ordinate bonds in BINAP must also be readily broken in the presence of a suitable donor. Evidence that this is the case comes from the observation that addition of acetonitrile to $[Ru(\eta^5\text{-}C_5H_5)\{(R)\text{-BINAP}\}]CF_3SO_3$ in CD_2Cl_2 immediately leads to loss of the η^2-co-ordination of the binaphthalene fragment. This is shown unambiguously by the loss of the high field aromatic signals in the ^{1}H NMR spectrum and by the large change in the ^{31}P NMR spectrum. A similar experiment with the weaker donor acetone in place of acetonitrile produced no significant changes in the NMR spectra of $[Ru(\eta^5\text{-}C_5H_5)\{(R)\text{-BINAP}\}]CF_3SO_3$. It was also found that the solid $[Ru(\eta^5\text{-}C_5H_5)\{(R)\text{-BINAP}\}]CF_3SO_3$ was slightly

TABLE 2. Selected bond lengths (Å) and angles (°) with estimated standard deviations (e.s.d.s) for $Ru(C_5H_5)\{(R)\text{-}(+)\text{-BINAP}\}I$ (**1**)

Bond lengths			
Ru(1)–I(1)	2.745(2)	Ru(1)–P(1)	2.317(4)
Ru(1)–P(2)	2.311(4)	Ru(1)–C(1)	2.214(12)
Ru(1)–C(2)	2.195(13)	Ru(1)–C(3)	2.210(12)
Ru(1)–C(4)	2.238(12)	Ru(1)–C(5)	2.240(12)
P(1)–C(6)	1.829(10)	P(1)–C(12)	1.852(10)
P(1)–C(18)	1.854(17)	P(2)–C(37)	1.839(17)
P(2)–C(38)	1.824(9)	P(2)–C(44)	1.873(9)
C(18)–C(19)	1.407(25)	C(18)–C(27)	1.357(21)
C(19)–C(20)	1.344(25)	C(20)–C(21)	1.427(22)
C(21)–C(22)	1.422(26)	C(21)–C(26)	1.425(22)
C(22)–C(23)	1.391(34)	C(23)–C(24)	1.303(30)
C(24)–C(25)	1.423(26)	C(25)–C(26)	1.377(23)
C(26)–C(27)	1.437(21)	C(27)–C(28)	1.457(20)
C(28)–C(29)	1.462(22)	C(28)–C(37)	1.412(21)
C(29)–C(30)	1.365(22)	C(29)–C(34)	1.418(23)
C(30)–C(31)	1.270(24)	C(31)–C(32)	1.455(28)
C(32)–C(33)	1.370(30)	C(33)–C(34)	1.473(26)
C(34)–C(35)	1.367(22)	C(35)–C(36)	1.377(23)
C(36)–C(37)	1.428(21)	C–C(cp)	1.420
C–C(phenyl)	1.395		
Bond angles			
I(1)–Ru(1)–P(1)	100.8(1)	I(1)–Ru(1)–P(2)	90.1(1)
P(1)–Ru(1)–P(2)	87.6(1)	Ru(1)–P(1)–C(6)	129.9(4)
Ru(1)–P(1)–C(12)	115.5(4)	C(6)–P(1)–C(12)	94.6(5)
Ru(1)–P(1)–C(18)	106.4(5)	C(6)–P(1)–C(18)	103.4(6)
C(12)–P(1)–C(18)	104.0(6)	Ru(1)–P(2)–C(37)	114.0(5)
Ru(1)–P(2)–C(38)	119.5(4)	C(37)–P(2)–C(38)	102.5(6)
Ru(1)–P(2)–C(44)	116.4(4)	C(37)–P(2)–C(44)	102.3(6)
C(38)–P(2)–C(44)	99.7(5)	P(1)–C(6)–C(7)	122.5(3)
P(1)–C(6)–C(11)	117.3(3)	P(1)–C(12)–C(13)	123.2(4)
P(1)–C(12)–C(17)	116.1(4)	P(1)–C(18)–C(19)	118.7(13)
P(1)–C(18)–C(27)	121.2(12)	C(19)–C(18)–C(27)	119.0(16)

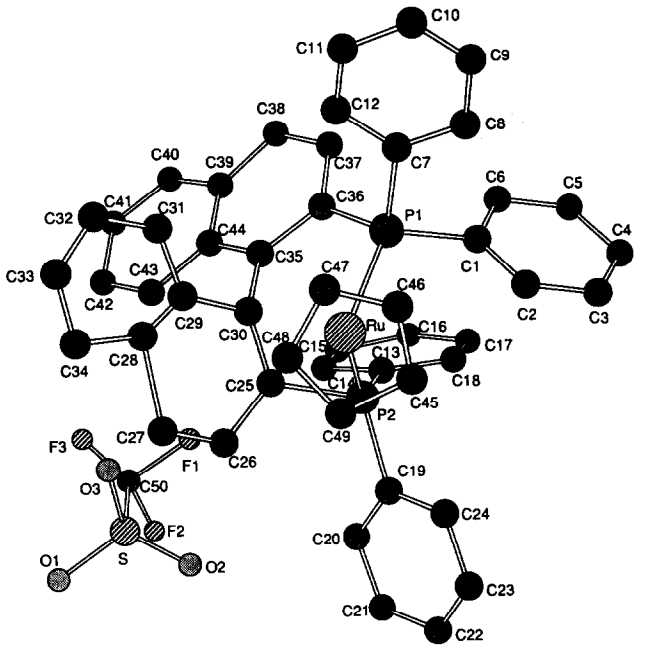

Fig. 2. Molecular structure of $[Ru(C_5H_5)\{(R)\text{-BINAP}\}]^+[CF_3SO_3]^-$ (2).

hygroscopic, which again may be due to the ready cleavage of the η^2-co-ordinate bonds of the binaphthalene fragment.

3. Experimental details

Microanalytical data were obtained by the University of Sheffield Microanalytical service. All reactions were carried out under nitrogen.

3.1. {(R)-2,2'-Bis(diphenylphosphino)-1,1'-binaphthyl}(cyclopentadienyl)iodoruthenium $Ru(\eta^5\text{-}C_5H_5)\{(R)\text{-BINAP}\}I$ (1)

Freshly cracked cyclopentadiene (3 mL, excess) was injected *via* a syringe into a refluxing solution of $Ru_3(CO)_{12}$ (231 mg, 0.36 mmol) in n-heptane (150 mL). The resulting red solution was heated under reflux for 2.5 h to give a pale yellow solution, which was then allowed to cool to room temperature. (+)-BINAP (675 mg, 1.08 mmol) was added to give a yellow suspension, which was then heated under reflux for 24 h to give a cloudy orange solution. The mixture was cooled to room temperature, CHI_3 (427 mg, 1.08 mmol) was added, and the mixture was stirred for 12 h at room temperature to give a red suspension. The solvent was removed under reduced pressure, and the crude product was chromatographed on silica gel (Merck 9385) with a mixture of dichloromethane–petroleum ether (4:1) as eluent. Evaporation of solvents from the eluate, gave a red crystalline product: m.p. 201–203 °C; yield 620 mg (63%). Recrystallisation from a mixture of dichloromethane–n-hexane–toluene afforded beautiful hexagonal, dark-red crystals of the desired product, which were found to be suitable for X-ray crystallography. Anal. Found: C, 63.4; H, 4.0; I, 13.4. $C_{49}H_{37}IP_2Ru \cdot 0.25CH_2Cl_2$ calc.: C, 63.1; H, 4.0; I, 13.5%. ^{1}H NMR (250 MHz, $CDCl_3$): δ 8.05–7.80 (m, 2 H, Ar*H*), 7.80–7.50 (m, 6 H, Ar*H*), 7.50–6.75 (overlapping m, 20 H, Ar*H*), 6.70–6.60 (m, 2 H, Ar*H*), 6.55 (d, $J = 7.5$ Hz, 1 H, Ar*H*), 6.25 (d, $J = 7.5$ Hz, 1 H, Ar*H*), 5.30 (s, CH_2Cl_2 solvent), 4.32 (s, 5 H, η^5-C_5H_5). $^{13}C\{^1H\}$ NMR (62.9 MHz, $CDCl_3$): δ 144.4–125.0 (m, 44 C, Ar*C*), 82.0 (s, 5 C, η^5-C_5H_5). $^{31}P\{^1H\}$ NMR (101 MHz, CD_2Cl_2): δ P_A 52.3, P_B 42.8 (AB q, $J_{PAPB} = 51.7$ Hz, 2P of BINAP). FAB-MS m/z 914 [M − H], 789 [M − I].

3.2. [{(R)-2,2'-Bis(diphenylphosphino)-1,1'-binaphthyl}(cyclopentadienyl)ruthenium(1 +)][triflate] [$Ru(\eta^5\text{-}C_5H_5)\{(R)\text{-BINAP}\}$][$CF_3SO_3$] (2)

$Ru(\eta^5\text{-}C_5H_5)\{(R)\text{-BINAP}\}I$ (360 mg, 0.4 mmol) was dissolved in dichloromethane (5 mL) to give a red solution. To this solution, CF_3SO_3Ag (110 mg, 0.4 mmol) was added at room temperature under argon. The mixture was stirred for 15 min to give a pale yellow suspension which was then filtered through a short column of Hiflow, the column subsequently being washed through with additional dichloromethane (10 mL). Removal of the solvent *in vacuo* gave pure product as a yellow solid: yield 330 mg (90%). Recrystallisation from dichloromethane–n-hexane gave pale yellow blocks suitable for X-ray structure determination. Anal. Found: C, 63.3; H, 4.0; S, 4.0. $C_{50}H_{37}F_3O_3P_2RuS \cdot 0.5H_2O$ calc.: C, 63.4; H, 4.0; S, 3.4%. ^{1}H NMR (400 MHz, CD_2Cl_2): δ 8.05–7.98 (m, 2 H, Ar*H*), 7.82–7.22 (m, 23 H, Ar*H*), 7.07 (d of d, $J = 6.0$ Hz, 1 H, Ar*H*), 6.77–6.71 (m, 1 H, Ar*H*), 6.38 (d, $J = 7.5$ Hz, 1 H, Ar*H*), 6.14–5.96 (m, 4 H, Ar*H*), 4.41 (s, 5 H, η^5-C_5H_5). $^{13}C\{^1H\}$ NMR (62.8 MHz, CD_2Cl_2): δ 145.2–125.9 (m, 44 C, Ar*C*), 88.3 (s, 5 C, η^5-C_5H_5). $^{31}P\{^1H\}$ NMR (101 MHz, CD_2Cl_2): δ P_A 74.0, P_B 14.1 (AB q, $J_{PAPB} = 43.7$ Hz, 2P of BINAP). $^{19}F\{^1H\}$ NMR (235 MHz, CD_2Cl_2): δ −78.8 (s, $CF_3SO_3^-$).

3.3. [Acetonitrile{(R)-2,2'-bis(diphenylphosphino)-1,1'-binaphthyl}(cyclopentadienyl)ruthenium(1 +)][triflate] [$Ru(\eta^5\text{-}C_5H_5)\{(R)\text{-BINAP}\}(NCCH_3)$]$CF_3SO_3$}

$[Ru(\eta^5\text{-}C_5H_5)\{(R)\text{-BINAP}\}]CF_3SO_3$ (30 mg) was dissolved in CD_2Cl_2 (0.5 mL) to give a yellow solution. To this solution, a drop of acetonitrile (13 mg) was added. No change in the colour of the solution was observed but NMR spectroscopy confirmed that com-

TABLE 3. Atom coordinates ($\times 10^4$) and temperature factors ($Å^2 \times 10^3$) for $[Ru(C_5H_5)\{(R)\text{-}(+)\text{-BINAP}\}]^+[CF_3SO_3]^-$ (2)

Atom	x	y	z	U_{eq} [a]
Ru(1)	134(1)	0	3442(1)	36(1)
P(1)	117(3)	1241(2)	4122(2)	36(1)
P(2)	141(3)	472(1)	1679(2)	38(1)
C(1)	1459(9)	1857(6)	3934(7)	40(4)
C(2)	2691(10)	1519(7)	4001(9)	54(4)
C(3)	3783(12)	1953(8)	3917(10)	70(5)
C(4)	3664(14)	2764(9)	3738(11)	83(6)
C(5)	2433(15)	3091(8)	3669(11)	83(6)
C(6)	1348(11)	2660(6)	3756(9)	54(5)
C(7)	223(9)	1384(6)	5621(7)	45(4)
C(8)	1368(12)	1671(7)	6373(8)	65(5)
C(9)	1457(12)	1780(7)	7514(9)	66(5)
C(10)	423(13)	1601(7)	7918(9)	68(5)
C(11)	−736(12)	1338(10)	7189(9)	90(6)
C(12)	−832(11)	1201(8)	6056(9)	76(5)
C(13)	−171(9)	1427(5)	1058(7)	40(4)
C(14)	−1411(12)	1615(7)	332(10)	63(5)
C(15)	−1640(12)	2317(7)	−211(9)	62(5)
C(16)	−599(12)	2860(6)	−19(10)	59(5)
C(17)	655(11)	2670(6)	669(8)	53(4)
C(18)	876(11)	1954(5)	1184(7)	46(4)
C(19)	969(8)	−12(8)	746(7)	45(3)
C(20)	360(11)	−64(9)	−406(8)	65(4)
C(21)	1048(19)	−383(8)	−1136(11)	93(7)
C(22)	2359(15)	−621(7)	−688(12)	83(7)
C(23)	2948(13)	−588(7)	419(11)	75(6)
C(24)	2278(11)	−283(6)	1176(10)	57(4)
C(25)	−1376(7)	−9(8)	1753(6)	38(3)
C(26)	−1796(10)	−737(6)	1176(8)	44(4)
C(27)	−2727(11)	−1154(6)	1446(9)	54(4)
C(28)	−3298(9)	−937(5)	2362(8)	39(4)
C(29)	−2968(9)	−217(5)	2907(7)	37(3)
C(30)	−2010(9)	300(5)	2579(7)	36(3)
C(31)	−3564(8)	−26(9)	3763(7)	53(3)
C(32)	−4438(11)	−525(7)	4098(10)	64(5)
C(33)	−4704(11)	−1227(8)	3585(10)	69(5)
C(34)	−4195(11)	−1441(7)	2725(11)	71(5)
C(35)	−2326(9)	1148(5)	2633(7)	34(3)
C(36)	−1471(8)	1660(5)	3387(7)	35(3)
C(37)	−1890(10)	2413(6)	3546(9)	52(4)
C(38)	−3097(10)	2712(6)	2890(8)	49(4)
C(39)	−3927(9)	2235(5)	2044(7)	38(3)
C(40)	−5124(9)	2510(6)	1316(8)	49(4)
C(41)	−5940(10)	2067(7)	529(9)	60(5)
C(42)	−5578(10)	1310(6)	398(9)	53(4)
C(43)	−4431(10)	1001(6)	1072(8)	48(4)
C(44)	−3562(9)	1451(5)	1928(7)	39(3)
C(45)	1940(14)	−734(9)	4205(14)	86(7)
C(46)	1500(16)	−417(7)	5041(12)	80(6)
C(47)	198(15)	−680(8)	4984(11)	72(6)
C(48)	−137(18)	−1144(9)	4083(15)	88(7)
C(49)	903(18)	−1221(8)	3565(11)	84(7)
C(50)	−4705(17)	785(10)	−2699(15)	129(9)
S(1)	−4204(5)	−150(3)	−2322(4)	113(2)
O(1)	−5158(11)	−622(7)	−3207(10)	132(6)
O(2)	−2920(12)	−183(11)	−2447(20)	279(14)
O(3)	−4410(24)	−219(10)	−1217(10)	252(13)
F(1)	−3993(16)	1301(7)	−1993(13)	210(8)
F(2)	−4587(22)	971(9)	−3695(11)	272(12)
F(3)	−5879(12)	925(10)	−2630(16)	270(11)

[a] Equivalent isotropic U defined as one third of the trace of the orthogonalised U_{ij} tensor.

TABLE 4. Selected bond lengths (Å) and bond angles (°) with estimated standard deviations (e.s.d.s) for $[Ru(C_5H_5)\{(R)\text{-}(+)\text{-}BINAP\}]^+[CF_3SO_3]^-$ (2)

Bond lengths			
Ru(1)–P(1)	2.327(3)	Ru(1)–P(2)	2.332(3)
Ru(1)–C(25)	2.258(7)	Ru(1)–C(30)	2.281(9)
Ru(1)–C(45)	2.275(14)	Ru(1)–C(46)	2.229(13)
Ru(1)–C(47)	2.232(14)	Ru(1)–C(48)	2.195(17)
Ru(1)–C(49)	2.272(15)	P(1)–C(1)	1.838(11)
P(1)–C(7)	1.844(10)	P(1)–C(36)	1.825(9)
P(2)–C(13)	1.829(10)	P(2)–C(19)	1.829(11)
P(2)–C(25)	1.827(10)	C(25)–C(26)	1.468(15)
C(25)–C(30)	1.464(14)	C(26)–C(27)	1.334(16)
C(27)–C(28)	1.467(16)	C(28)–C(29)	1.426(12)
C(28)–C(34)	1.447(17)	C(29)–C(30)	1.488(13)
C(29)–C(31)	1.409(14)	C(30)–C(35)	1.524(13)
C(31)–C(32)	1.407(18)	C(32)–C(33)	1.374(18)
C(33)–C(34)	1.367(19)	C(35)–C(36)	1.422(12)
C(35)–C(44)	1.456(12)	C(36)–C(37)	1.418(14)
C(37)–C(38)	1.410(14)	C(38)–C(39)	1.435(13)
C(39)–C(40)	1.420(12)	C(39)–C(44)	1.439(13)
C(40)–C(41)	1.354(14)	C(41)–C(42)	1.398(16)
C(42)–C(43)	1.379(13)	C(43)–C(44)	1.433(12)
C(45)–C(46)	1.359(24)	C(45)–C(49)	1.440(21)
C(46)–C(47)	1.429(23)	C(47)–C(48)	1.345(21)
C(48)–C(49)	1.415(28)		
Bond angles			
P(1)–Ru(1)–P(2)	90.6(1)	P(1)–Ru(1)–C(25)	105.6(3)
P(2)–Ru(1)–C(25)	46.9(3)	P(1)–Ru(1)–C(30)	81.5(2)
P(2)–Ru(1)–C(30)	74.5(3)	C(25)–Ru(1)–C(30)	37.6(3)
Ru(1)–P(1)–C(1)	114.7(4)	Ru(1)–P(1)–C(7)	119.0(3)
C(1)–P(1)–C(7)	102.0(4)	Ru(1)–P(1)–C(36)	106.8(3)
C(1)–P(1)–C(36)	109.5(4)	C(7)–P(1)–C(36)	104.2(5)
Ru(1)–P(2)–C(13)	132.0(3)	Ru(1)–P(2)–C(19)	123.2(4)
C(13)–P(2)–C(19)	102.6(5)	Ru(1)–P(2)–C(25)	64.4(2)
C(13)–P(2)–C(25)	112.4(5)	C(19)–P(2)–C(25)	112.9(5)
Ru(1)–C(25)–P(2)	68.7(3)	Ru(1)–C(25)–C(26)	120.0(7)
P(2)–C(25)–C(26)	121.8(7)	Ru(1)–C(25)–C(30)	72.0(4)
P(2)–C(25)–C(30)	115.7(8)	C(26)–C(25)–C(30)	121.7(9)
C(25)–C(26)–C(27)	119.8(10)	C(26)–C(27)–C(28)	122.2(9)
C(27)–C(28)–C(29)	119.6(9)	C(27)–C(28)–C(34)	121.2(9)
C(29)–C(28)–C(34)	119.1(10)	C(28)–C(29)–C(30)	120.2(9)
C(28)–C(29)–C(31)	117.6(10)	C(30)–C(29)–C(31)	122.2(9)
Ru(1)–C(30)–C(25)	70.3(5)	Ru(1)–C(30)–C(29)	112.9(5)
C(25)–C(30)–C(29)	115.8(8)	Ru(1)–C(30)–C(35)	113.7(5)
C(25)–C(30)–C(35)	122.3(9)	C(29)–C(30)–C(35)	114.0(8)
C(29)–C(31)–C(32)	122.2(12)	C(31)–C(32)–C(33)	119.0(12)
C(32)–C(33)–C(34)	122.0(12)	C(28)–C(34)–C(33)	120.0(11)
C(30)–C(35)–C(36)	122.2(7)	C(30)–C(35)–C(44)	119.8(7)
C(36)–C(35)–C(44)	118.0(8)	P(1)–C(36)–C(35)	114.0(7)
P(1)–C(36)–C(37)	125.4(6)	C(35)–C(36)–C(37)	120.6(8)
C(36)–C(37)–C(38)	122.0(9)	C(37)–C(38)–C(39)	118.7(9)
C(38)–C(39)–C(40)	121.7(9)	C(38)–C(39)–C(44)	119.9(8)
C(40)–C(39)–C(44)	118.3(8)	C(39)–C(40)–C(41)	122.9(10)
C(40)–C(41)–C(42)	119.0(9)	C(41)–C(42)–C(43)	121.4(9)
C(42)–C(43)–C(44)	120.8(9)	C(35)–C(44)–C(39)	120.4(8)
C(35)–C(44)–C(43)	122.1(8)	C(39)–C(44)–C(43)	117.5(8)
C(46)–C(45)–C(49)	107.2(14)	C(45)–C(46)–C(47)	110.5(12)
C(46)–C(47)–C(48)	105.5(15)	C(47)–C(48)–C(49)	111.8(15)
C(45)–C(49)–C(48)	105.0(13)		

plete reaction had occurred. ^{1}H NMR (400 MHz, CD_2Cl_2): δ 7.76 (d, $J = 8.5$ Hz, 1 H, ArH), 7.69 (d, $J = 8.5$ Hz, 1 H, ArH), 7.62 (d, $J = 8.5$ Hz, 1 H, ArH), 7.53–6.93 (overlapping m, 25 H, ArH), 6.75 (m, 2 H, ArH), 6.62 (d, $J = 8.5$ Hz, 1 H, ArH), 6.25 (d, $J = 8.5$ Hz, 1 H, ArH), 4.40 (s, 5 H, η^5-C_5H_5). ^{31}P{^{1}H} NMR (101 MHz, CD_2Cl_2): δ P_A 55.03 P_B 46.6(AB q, J_{PAPB} = 46.5 Hz, 2P of BINAP). ^{19}F{^{1}H} NMR (235 MHz, CD_2Cl_2): δ −78.9 (s, $CF_3SO_3^-$).

3.4. Crystal data

3.4.1. $Ru(C_5H_5)\{(R)\text{-}BINAP\}I \cdot PhCH_3$ (1)

$C_{56}H_{45}IP_2Ru$; $M = 1007.82$, crystallises from toluene as dark red hexagons. Rhombohedral, a = 14.882(5) Å, $\alpha = 89.751(30)°$, $U = 3296(4)$ Å^3, $Z = 3$, $D_c = 1.523$ g cm^{-3}, space group $R3$ (C_3^4, No. 146), Mo-Kα radiation ($\bar{\lambda} = 0.71069$ Å), μ(Mo-Kα) = 11.53 cm^{-1}, $F(000) = 1523.84$.

3.4.2. $[Ru(\eta^5\text{-}C_5H_5)\{(R)\text{-}(BINAP)\}]CF_3SO_3$ (2)

$C_{50}H_{37}F_3O_3P_2RuS$; $M = 937.92$, crystallises from dichloromethane–n-hexane as yellow blocks; crystal dimensions 0.55 × 0.25 × 0.20 mm. Monoclinic, a = 10.518(9), b = 17.467(9), c = 12.364(11) Å, β = 105.63(6)° $U = 2187.5(27)$ Å^3, $Z = 2$, $D_c = 1.424$ g cm^{-3}, space group $P2_1$ (C_2^2, No. 4), Mo-Kα radiation ($\bar{\lambda}$ = 0.71069 Å), μ(Mo-Kα) = 5.21 cm^{-1}, $F(000) = 955.90$.

3.5. Structure analysis and refinement

Three-dimensional, room temperature X-ray data were collected on a Nicolet R3 diffractometer by the omega scan method in the range $3.5 < 2\theta < 50°$ and $3.5 < 2\theta < 45°$ for **1** and **2**, respectively.

For **1** the 4578 independent reflections (of 8853 measured) for which $|F|/\sigma(|F|) > 3.0$ were corrected for Lorentz and polarisation effects, and for absorption by analysis of 10 azimuthal scans (minimum and maximum transmission coefficients 0.31 and 0.39). The structure was solved by Patterson and Fourier techniques and refined by blocked cascade least squares methods. The five membered ring and the four terminal phenyl rings were refined with constrained D_{5h} and D_{6h} geometries, respectively. A molecule of toluene of solvation was refined as a rigid group, then fixed in position for the final cycles to aid convergence. Hydrogen atoms were included in calculated positions and refined in riding mode. Refinement converged at a final $R = 0.0924$, ($R_w = 0.0970$, 421 parameters, mean and maximum δ/σ 0.062, 0.212), with allowance for the thermal anisotropy of all non-hydrogen atoms, with the exception of the atoms of the solvent which were given a common isotropic thermal parameter. The correct enantiomeric form of the BINAP fragment was confirmed by the lower value of R (by 0.0022). Minimum and maximum final electron density −1.02 and 2.33 e Å^{-3} (near to iodine and ruthenium, and to the solvent). A weighting scheme $w^{-1} = \sigma^2(F) + 0.00300 \cdot (F)^2$ was used in the latter stages of refinement.

For **2** the 2595 independent reflections (of 3179 measured) for which $|F|/\sigma(|F|) > 3.0$ were corrected for Lorentz and polarisation effects, and for absorption by analysis of 4 azimuthal scans (minimum and maximum transmission coefficients 0.690 and 0.753). The structure was solved by direct methods and refined by blocked cascade least squares methods. Hydrogen atoms were included in calculated positions and refined in riding mode. Refinement converged at a final $R = 0.0509$, ($R_w = 0.0498$, 540 parameters, mean and maximum δ/σ 0.005, 0.020), with allowance for the thermal anisotropy of all non-hydrogen atoms. Minimum and maximum final electron density −0.42 and 0.49 e A^{-3}. A weighting scheme $w^{-1} = \sigma^2(F) + 0.00109 \cdot (F)^2$ was used in the latter stages of refinement. The known enantiomeric form of the BINAP ligand was confirmed by the lower R (by 0.0007) of the reported structure.

In each case complex scattering factors were taken from the program package SHELXTL [15] as implemented on the Data General DG30 computer.

A full list of bond lengths and bond angles with estimated standard deviations, a list of anisotropic thermal vibrational parameters and a table of predicted hydrogen atom coordinates have been deposited at the Cambridge Crystallographic Data Centre.

Acknowledgements

We wish to record our sincere thanks to the S.E.R.C. for a research fellowship (to D.D.P.), to Johnson Matthey for the generous loan of ruthenium trichloride (to C.W.) and to the Royal Society and the S.E.R.C. for funds for the X-ray and computing equipment.

References

1 (a) R. Noyori, *Chem. Soc. Rev., 18* (1989) 187; (b) R. Noyori and H. Takaya, *Acc. Chem. Res., 23* (1990) 345; (c) R. Noyori, *Chemtech., 22* (1992) 360.
2 T. Manimaran, T.-C. Wu, W.D. Klobucar, C.H. Kolich, G.P. Stahley, F.R. Fronczek and S.E. Watkins, *Organometallics, 12* (1993) 1467 and references therein.
3 P. Krasik and H. Alper, *Tetrahedron: Asymmetry, 3* (1992) 1283.
4 H. Takaya, T. Ohta, N. Sayo, H. Kumobayashi, S. Akutagawa, S. Inoue, I. Kasahara and R. Noyori, *J. Am. Chem. Soc., 109* (1987) 1596 and 4129.

5 E. Cesarotti, P. Antognazza, A. Mauri, M. Pallavicini and L. Villa, *Helv. Chim. Acta, 75* (1992) 2563.
6 R. Noyori, T. Ohkuma, M. Kitamura, H. Takaya, N. Sayo, H. Kumobayashi and S. Akutagawa, *J. Am. Chem. Soc., 109* (1987) 5856.
7 J.B. Hoke, S.L. Hollis and E.W. Stern, *J. Organomet. Chem., 455* (1993) 193.
8 C. White and E. Cesarotti, *J. Organomet. Chem., 287* (1985) 123.
9 R.J. Kulawiec, J.W. Faller and R.H. Crabtree, *Organometallics, 9* (1990) 745 and references therein.
10 K. Mashima, K. Kusano, T. Ohta, R. Noyori and H. Takaya, *J. Chem. Soc., Chem. Commun.*, (1989) 1208.
11 (a) T. Ohta, H. Takaya and R. Noyori, *Inorg. Chem., 27* (1988) 566; (b) H. Kuwano, Y. Ishii, T. Kodama, M. Suburi and Y. Uchida, *Chem. Lett.*, (1987) 1311; (c) M.T. Ashby, M.A. Khan and J. Halpern, *Organometallics, 10* (1991) 2011 and references therein.
12 R.M. Chin, L. Dong, S.B. Duckett, M.G. Partridge, W.D. Jones and R.N. Perutz, *J. Am. Chem. Soc., 115* (1993) 7685 and references therein.
13 (a) T. Tsukahara, H. Kawano, Y. Ishii, T. Takahashi, M. Saburi, Y. Uchida and S. Akutagawa, *Chem. Lett.*, (1988) 2055; (b) M. Saburi, M. Ohnuki, M. Ogasawara, T. Takahashi and Y. Uchida, *Tetrahedron Lett., 33* (1992) 5783.
14 M. Brookhart, A.F. Volpe Jr., D.M. Lincoln, I.T. Horváth and J.M. Millar, *J. Am. Chem. Soc., 112* (1990) 5634 and references therein.
15 G.M. Sheldrick, SHELXTL, an integrated system for solving, refining and displaying crystal structures from diffraction data (Revision 5.1), University of Göttingen, Germany, 1985.